J|A|C|S
ARTICLES
Published on Web 01/23/2007

Ordered Mesoporous Silicas and Carbons with Large Accessible Pores Templated from Amphiphilic Diblock Copolymer Poly(ethylene oxide)-*b*-polystyrene

Yonghui Deng,[†,‡] Ting Yu,[†] Ying Wan,[†] Yifeng Shi,[†] Yan Meng,[†] Dong Gu,[†] Lijuan Zhang,[†] Yan Huang,[†] Chong Liu,[†] Xiaojing Wu,[‡] and Dongyuan Zhao*[,†]

Contribution from the Department of Chemistry, Shanghai Key Laboratory of Molecular Catalysis and Innovative Materials, Key Laboratory of Molecular Engineering of Polymers and Laboratory of Advanced Materials and the Department of Materials Science, Fudan University, Shanghai 200433, People's Republic of China

Received October 14, 2006; E-mail: dyzhao@fudan.edu.cn

Abstract: Highly ordered mesoporous carbons and silicas with ultralarge accessible pores have been successfully synthesized by using laboratory-made poly(ethylene oxide)-*b*-polystyrene (PEO-*b*-PS) diblock copolymers as templates via the evaporation-induced self-assembly (EISA) approach. Resols and tetraethyl orthosilicate (TEOS) serve as carbon and silica precursors, respectively. Small-angle X-ray scattering (SAXS) and transmission electron microscopy (TEM) measurements show that the mesoporous carbons (denoted as C-FDU-18) possess face centered cubic closed-packing (*fcc*) mesostructure ($Fm\bar{3}m$) with large-domain ordering. N_2 sorption isotherms reveal a large mesopore at the mean value of 22.6 nm with a narrow pore-size distribution. Mesoporous silicas (Si-FDU-18) also display a highly ordered *fcc* closed-packing mesostructure with an ultralarge unit cell ($a = 54.6$ nm). A hydrothermal recrystallization was introduced for the first time to produce micropores in thick silica walls (~7.7 nm) and thus to generate ultralarge accessible mesopores (30.8 nm). Notably, the amphiphilic diblock copolymer with high molecular weight (PEO_{125}-PS_{230}, 29700 g mol^{-1}) in this report was prepared via a simple method of atom transfer radical polymerization (ATRP). It can be easily available for chemists even without any experience in polymer synthesis.

1. Introduction

Ordered mesoporous materials with large pore sizes have received much attention because of their potential applications involved with large molecules, in adsorption, separation, nanodevice, photonic waveguide, encapsulation of proteins and catalysis.[1,2] Great efforts are therefore focused on mesoporous materials with large accessible pores. A variety of synthetic strategies have been developed on the basis of poly(ethylene oxide)-*b*-poly(propylene oxide)-*b*-poly(ethylene oxide) (PEO-PPO-PEO) triblock copolymers as templates. Many ordered large-pore mesoporous silicas were obtained,[3−9] for example, SBA-15,[3] SBA-16,[4] FDU-5,[5] FDU-12,[7] KIT-5,[8] and KIT-6.[9] The commercially available PEO-PPO-PEO triblock copolymers themselves have few chances to directly template ordered mesoporous silicas with pore sizes larger than 12 nm because of the limitation of molecular weight and composition.[8−10] The main strategy to expand the pores is the adding of swelling agents, for example, 1,3,5-trimethylbenzene (TMB) and *n*-butanol. However, it sometimes results in disordered mesostructures, such as silica mesocellular foams (MCF).[11,12] To date, the largest accessible pore size of ordered mesoporous silica is limited to 27 nm by using PEO-PPO-PEO as a template, even with the assistance of TMB via a low-temperature route.[7] Besides that, high-molecular-weight copolymers with long hydrophobic segments become promising candidates to template large-pores mesoporous silicates since the pore dimensions are primarily related with the molecular weights of hydrophobic segments.[13−18] Templin et al.[19] first used poly(isoprene)-*b*-poly(ethylene oxide) (PI-PEO) block copolymers with high molec-

[†] Department of Chemistry, and Shanghai Key Laboratory of Molecular Catalysis and Innovative Materials, Key Laboratory of Molecular Engineering of Polymers, Laboratory of Advanced Materials.
[‡] Department of Materials Science.

(1) Estermann, M.; McCusker, L. B.; Baeriocher, C.; Merroche, A.; Kessier, H. *Nature* **1991**, *352*, 320.
(2) Fan, J.; Shui, W.; Yang, P.; Wang, X.; Xu, Y.; Wang, H.; Chen, X.; Zhao, D. *Chem.—Eur. J.* **2005**, *11*, 5391.
(3) Zhao, D.; Feng, J.; Huo, Q.; Melosh, N.; Fredrickson, G. H.; Chmelka, B. F.; Stucky, G. D. *Science* **1998**, *279*, 548.
(4) Zhao, D.; Huo, Q.; Feng, J.; Chmelka, B. F.; Stucky, G. D. *J. Am. Chem. Soc.* **1998**, *120*, 6024.
(5) Liu, X.; Tian, B.; Yu, C.; Gao, F.; Xie, S.; Tu, B.; Che, R.; Peng, L.; Zhao, D. *Angew. Chem., Int. Ed.* **2002**, *41*, 3876.
(6) Yu, C.; Yu, Y.; Zhao, D. *Chem. Commun.* **2000**, 575.
(7) Fan, J.; Yu, C.; Lei, J.; Zhang, Q.; Li, T.; Tu, B.; Zhou, W.; Zhao, D. *J. Am. Chem. Soc.* **2005**, *127*, 10794.
(8) Kleitz, F.; Liu, D.; Anilkumar, G. M.; Park, I. S.; Solovyov, L. A.; Shmakov, A. N.; Ryoo, R. *J. Phys. Chem. B* **2003**, *107*, 14296.
(9) Kleitz, F.; Choi, S. H.; Ryoo, R. *Chem. Commun.* **2003**, 2136.
(10) Chen, D. H.; Li, Z.; Yu, C. Z.; Shi, Y. F.; Zhang, Z.; Tu, B.; Zhao, D. Y. *Chem. Mater.* **2005**, *17*, 3228.
(11) Schmidt-Winkel, P.; Lukens, W. W., Jr.; Zhao, D.; Yang, P.; Chmelka, B. F.; Stucky, G. D. *J. Am. Chem. Soc.* **1999**, *121*, 254.
(12) Kim, S. S.; Pauly, T. R.; Pinnavaia, T. J. *Chem. Commun.* **2000**, 1661.
(13) Kramer, E.; Forster, S.; Goltner, C.; Antonietti, M. *Langmuir* **1998**, *14*, 2027.
(14) Yu, K.; Hurd, A. J.; Eisenberg, A.; Brinker, C. J. *Langmuir* **2001**, *17*, 7961.

10.1021/ja067379v CCC: $37.00

ular weight (M_w = 34 kg mol^{-1}) to prepare mesostructured aluminosilicate−polymer composites with ordered length scales up to 40 nm. However, the removal of the copolymer templates to generate accessible mesopores was not reported. By using high-molecular-weight polystyrene-*b*-poly(ethylene oxide) copolymer (PS_{215}-PEO_{100}, M_w = 27 kg mol^{-1}), Yu and co-workers[14−16] synthesized ordered mesoporous silicates with large cell parameters. Unfortunately, the mesopores were isolated owing to the spherical packing of templates and the gradual retraction of PEO segments during the formation of PS-*b*-PEO/silica mesostructures. The large pores could not be opened, and no specific BET surface area could be detected by N_2 sorption isotherms. A strategy to get large accessible pores is much in demand.

In recent years, ordered mesoporous carbons have attracted increasing interests because of their unique characters including excellent stability, high surface areas, and so on. These features make them prospective candidates as hydrogen-storage adsorbents, catalysts, electrode materials, and even hard templates for the synthesis of nanostructured materials, etc. The synthesis of ordered mesoporous carbons was first realized from Ryoo and co-workers[20] by using ordered mesoporous silicas as hard templates, which have greatly stimulated research interests in the mesostructured material community. However, the method is fussy and costly. In addition, their mesopores are originated from the pore walls of silica templates. Seldom cases can tune the wall thickness in a large range. Consequently, the pore sizes are rather small.[21] More recently, the organic−organic self-assembly[22−26] approach has been successfully used to synthesize ordered mesoporous carbon frameworks, similar to the inorganic−organic assembly for mesoporous silicas. A family of carbon mesostructures, including two-dimensional (2-D) hexagonal (space group of *p*6*m*), 3-D bicontinuous ($Ia\bar{3}d$), body-centered cubic ($Im\bar{3}m$) and lamellar symmetries, was prepared by using phenolic resins as a carbon source and triblock copolymers PEO-PPO-PEO as templates. However, the pore sizes of mesoporous carbons are limited by the molecular weight copolymers, the same as mesoporous silicas. Moreover, the large structural shrinkage during the pyrolysis and carbonization leads to the pore sizes lower than 4 nm.[24,25] A triconstituent co-assembly strategy has been developed to incorporate rigid components such as inorganic silicates into carbon frameworks to reduce the shrinkage.[27,28] The pore sizes of obtained mesoporous carbons can only be enlarged to about 6 nm. Reminiscent to the research on mesoporous silicates, the design of high-molecular-weight copolymers is feasible for the synthesis of large-pore mesoporous carbons.

Herein, we report a rational synthesis of highly ordered mesoporous carbons and silicas with ultralarge accessible pores by using laboratory-made poly(ethylene oxide)-*b*-polystyrene (PEO-*b*-PS) diblock copolymers as templates via the evaporation-induced self-assembly (EISA) approach. Resols and tetraethyl orthosilicate (TEOS) serve as carbon and silica precursors, respectively. Small-angle X-ray scattering (SAXS) and transmission electron microscopy (TEM) measurements show that the mesoporous carbons (denoted as C-FDU-18) possess face centered cubic closed-packing (*fcc*) mesostructure ($Fm\bar{3}m$) with large-domain ordering. N_2 sorption isotherms reveal a large mesopore at the mean value of 22.6 nm with a narrow pore size distribution. Mesoporous silicas (Si-FDU-18) also display a highly ordered *fcc* closed-packing mesostructure with ultralarge unit cell (a = 54.6 nm). A hydrothermal recrystallization was introduced for the first time to produce micropores in thick silica walls (~7.7 nm), and thus to generate ultralarge accessible mesopores (30.8 nm). Notably, the amphiphilic diblock copolymer with high molecular weight (PEO_{125}-PS_{230}, 29700 g mol^{-1}) in this report was prepared via a simple method of atom transfer radical polymerization (ATRP).[29] It can be easily available for chemists even without any experience in polymer synthesis.

2. Experimental Section

2.1. Chemicals. Monomethoxy poly(ethylene oxide) (monomethoxy-PEO5000), 2-bromoisobutyryl bromide and *N*,*N*,*N*′,*N*′,*N*″-pentamethyldiethylenetriamine (PMDETA) were purchased from Acros Corp. Tetrahydrofuran (THF), pyridine, styrene, ether, CuBr, petroleum ether (60−90 °C), tetraethyl orthosilicate (TEOS), phenol, formalin solution (37 wt %), NaOH, and HCl were purchased from Shanghai Chemical Corp. Styrene was purified by filtrating through Al_2O_3 column. All other chemicals were used as received. Deionized water was used for all experiments. The resol precursors with low-molecule-weight (M_w < 500) were prepared according to a procedure reported previously.[24]

2.2. Preparation of PEO-*b*-PS Diblock Copolymer. The diblock copolymer was prepared by a simple ATRP method involving two steps. The first step was the synthesis of macroiniator PEO-Br. An amount of 20.0 g of monomethoxy PEO5000 was dissolved in 60 mL of THF. Then 40 mL of pyridine was added to obtain a homogeneous solution. The solution was cooled in ice-water bath. To it, 3.00 g of 2-bromoisobutyryl bromide (13 mmol) was added dropwise under stirring for 30 min. The resultant solution was further stirred at 30 °C overnight. After cooling to room temperature, 200 mL of cold ether was added to the solution. The white product of PEO-Br was precipitated from the reaction solution. It was washed with cold ether and further dried in vacuum. In the second step, 3.00 g of PEO-Br (0.53 mmol), 0.08 g of CuBr (0.57 mmol), 0.10 g of PMDETA (0.57 mmol), and 15.0 g of styrene (144 mmol) were added to an ampoules bottle. The bottle, containing reactants, was fully degassed with three freeze−pump−thaw cycles and sealed under vacuum. It was subsequently immersed in a thermostated oil bath at 110 °C under stirring to allow polymerization of styrene. The reaction continued for 3 h after which the system was cooled down to room temperature. The gel-like product was dissolved by 50 mL of THF and filtered through Al_2O_3 column to remove Cu complex. Petroleum ether (200 mL) was poured into the solution to precipitate PEO-*b*-PS block copolymer. The copolymer was then dried in vacuum. The yield was 67 wt % on the basis of initial styrene amount.

(15) Smarsly, B.; Xomeritakis, G.; Yu, K.; Liu, N.; Fan, H.; Roger, A.; Assink, R. A.; Drewien, C. A.; Ruland, W.; Brinker, C. J. *Langmuir* **2003**, *19*, 7295.
(16) Yu, K.; Smarsly, B.; Brinker, C. J. *Adv. Funct. Mater.* **2003**, *13*, 47.
(17) Thomas, A.; Schlaad, H.; Smarsly, B.; Antonietti, M. *Langmuir* **2003**, *19*, 4455.
(18) Groenewolt, M.; Brezesinski, T.; Schlaad, H.; Antonietti, M.; Groh, P. W.; Ivan, B. *Adv. Mater.* **2005**, *17*, 1158.
(19) Templin, M.; Franck, A.; Chesne, A. D.; Leist, H.; Zhang, Y.; Ulrich, R.; Schadler, V.; Wiesner, U. *Science* **1997**, *278*, 1795.
(20) Ryoo, R.; Joo, S. H.; Jun, S. *J. Phys. Chem. B* **1999**, *103*, 7743.
(21) Kim, T. W.; Solovyov, L. A. *J. Mater. Chem.* **2006**, *16*, 1445.
(22) Liang, C.; Hong, K.; Guiochon, G. A.; Mays, J. M.; Dai, S. *Angew. Chem., Int. Ed.* **2004**, *43*, 5785.
(23) Tanaka, S.; Nishiyama, N.; Egashira, Y.; Ueyama, K. *Chem. Commun.* **2005**, 2125.
(24) Meng, Y.; Gu, D.; Zhang, F.; Shi, Y.; Yang, H.; Tu, B.; Yu, C.; Zhao, D. *Angew. Chem., Int. Ed.* **2005**, *44*, 7053.
(25) Meng, Y.; Gu, D.; Zhang, F.; Shi, Y.; Cheng, L.; Feng, D.; Wu, Z.; Chen, Z.; Wan, Y.; Stein, A.; Zhao, D. *Chem. Mater.* **2006**, *18*, 4447.
(26) Zhang, F.; Meng, Y.; Gu, D.; Yan, Y.; Yu, C.; Tu, B.; Zhao, D. *J. Am. Chem. Soc.* **2005**, *127*, 13508.
(27) Liu, R.; Shi, Y.; Wan, Y.; Meng, Y.; Zhang, F.; Gu, D.; Chen, Z.; Tu, B.; Zhao, D. *J. Am. Chem. Soc.* **2006**, *128*, 11652.
(28) Wan, Y.; Yang, H.; Zhao, D. *Acc. Chem. Res.* **2006**, *39*, 423.
(29) Wang, J.; Matyjaszewski, K. *J. Am. Chem. Soc.* **1995**, *117*, 5614.

2.3. Synthesis of Mesoporous Carbons (C-FDU-18). Mesoporous carbons were prepared through an EISA strategy by using the diblock copolymer PEO-*b*-PS as a template, THF as a solvent, resols as a carbon source. For a typical synthesis, 2.00 g of the resol precursor in THF solution (20 wt %, containing 0.25 g phenol and 0.15 g formaldehyde) was added to 5.0 g of THF solution of PEO-*b*-PS (2.0 wt %, containing 0.10 g copolymer) with stirring to form a homogeneous solution. Transparent films were obtained by pouring the solution into Petri dishes to evaporate THF at room temperature for 12 h, followed by further heating in an oven at 100 °C for 24 h. The as-made product was scraped and crushed into powders. Pyrolysis was carried out in a tubular furnace under N_2 at different temperatures (450−900 °C) for 3 h. The heating rate was 1 °C/min below 450 °C and 5 °C/min above 600 °C. Samples pyrolyzed at 450, 800, and 900 °C correspond to the products of C-FDU-18-450, C-FDU-18-800 and C-FDU-18-900, respectively.

2.4. Synthesis of Mesoporous Silica (Si-FDU-18). Mesoporous silicas were also prepared through an EISA strategy in THF by using PEO-*b*-PS copolymer as a template and TEOS as a silica precursor. Besides subsequent direct calcination, a hydrothermal treatment was adopted before it. In a typical synthesis procedure, 1.00 g of TEOS and 0.30 g of 0.1 M HCl solution were added to 5.00 g of THF solution of PEO-*b*-PS (2.0 wt %, containing 0.10 g copolymer) with stirring for 30 min to form a homogeneous solution. It was poured into Petri dishes to evaporate THF at room temperature for 48 h. The transparent films were collected and grounded into powders. Then the powders were transferred into an autoclave containing 30 mL HCl solution (1.0 M) and hydrothermally heated at 100 °C for 3 days. The product (Si-FDU-18-H) was washed with water, dried at room temperature, and calcined in air at 600 °C for 6 h to produce Si-FDU-18-HC with white color. It is noted that plentiful air or a longer calcination time was required, otherwise, the calcined sample with a little yellow tint would be obtained. The sample Si-FDU-18-C was obtained by direct calcination of as-made Si-FDU-18 in air at 600 °C for 6 h. Both of the above calcinations were conducted in a furnace with a heating rate of 1 °C/min.

2.5. Characterization and Measurements. ^{1}H NMR spectra were recorded at 25 °C on a DMX 500-MHz spectrometer (Bruker, Germany) with tetramethylsilane as an internal standard and $CDCl_3$ as a solvent. GPC was performed on an Agilent 1100 gel permeation chromatographer with refractive index detector and UV−vis detector (wavelength 190−950 nm) by the use of THF as an eluent (1.0 mL/min). GPC was calibrated with monodispersed polystyrene standards. Fourier-transform infrared (FTIR) spectra were collected on a Nicolet Fourier spectrophotometer using KBr pellets. Thermogravimetric analysis (TGA) was carried out using a Mettler Toledo TGA-SDTA851 analyzer (Switzerland) from 25 to 600 °C (or 900 °C) under nitrogen or air with a heating rate of 5 °C/min. SAXS measurements were taken on a Nanostar U small-angle X-ray scattering system (Bruker, Germany) using Cu Kα radiation (40 kV, 35 mA). The *d*-spacing values were calculated by the formula $d = 2\pi/q$. The wall thickness was calculated from $W_T = \sqrt{2}a/2 - D$, where a represents the cell parameter and D is the pore diameter calculated from the N_2 sorption measurement. Nitrogen sorption isotherms were measured at 77 K with a Micromeritics Tristar 3000 analyzer. Before measurements, the samples were degassed in a vacuum at 200 °C for at least 6 h. The Brunauer−Emmett−Teller (BET) method was utilized to calculate the specific surface areas. By using the Broekoff−de Boer (BdB) sphere model,[30] the pore volumes and pore size distributions were derived from the adsorption branches of isotherms, and the total pore volumes (V_t) were estimated from the adsorbed amount at a relative pressure P/P_0 of 0.992. The calibration curve was obtained by using the carbon black (part no. 004-16833-00) as a reference material and nitrogen as an adsorption gas. TEM experiments were conduced on a JEOL 2011 microscope (Japan) operated at 200 kV. ^{29}Si solid-state NMR experiments were performed on a Bruker DSX300 spectrometer (Germany) under conditions of cross polarization (CP) and magic-angle sample spinning (MAS). The spectra were collected at room temperature with a frequency of 59.6 MHz, a recycling delay of 600 s, a radiation frequency intensity of 62.5 kHz, and a reference sample of Q_8M_8 ($[(CH_3)_3SiO]_8Si_8O_{12}$). Raman spectra were obtained with a Dilor LabRam-1B microscopic Raman spectrometer (France), using a He−Ne laser with an excitation wavelength of 632.8 nm. The C, H, and O contents were measured on a Vario EL III elemental analyzer (Germany).

3. Results and Discussion

3.1. Synthesis of PEO-*b*-PS Diblock Copolymer. The synthetic procedure of PEO-*b*-PS (**M2**) simply involves two steps, that is, the preparation of macroinitiator (**M1**) by reacting monomethoxy PEO (5000) with 2-bromoisobutyrl bromide, and the polymerization of styrene (Figure 1A). The successful preparation of PEO-Br and PEO-*b*-PS was verified by FT-IR spectra (Supporting Information, SI, Figure S1) and ^{1}H NMR spectra (Figure 1B). The signals around 3.60 and 2.45 ppm of **M1** are attributed to EO units and -CH_3 from 2-bromoisobutyrl bromide, respectively. In addition, the signals at 1.20−1.63 and 6.29−7.22 ppm for diblock copolymer PEO-*b*-PS (**M2**) are ascribed to the styrene unit. The Mn values of **M1** and **M2** calculated from ^{1}H NMR data are about 5700 and 29700 g mol^{-1}, respectively. Therefore, the composition of this diblock copolymer can be approximately formulated as PEO_{125}-PS_{230}. Gel permeation chromatography (GPC) (Figure 1C) shows a polydispersity index (PDI) of 1.17, indicating a narrow molecular-weight distribution. The TGA (Figure S2) of PEO-*b*-PS diblock copolymer shows a weight loss of about 97 wt % in the temperature range of 310 to 450 °C under N_2 and 98 wt % in 250−350 °C under air. It implies that the template can be easily removed by pyrolysis both in N_2 and air.

3.2. Large-Pore Ordered Mesoporous Carbons (C-FDU-18). Diblock copolymer PEO_{125}-PS_{230} is insoluble in water or ethanol owing to the high molecular weight of the PS segment. Therefore, the EISA approach in THF was employed to synthesize mesoporous carbon and silica FDU-18. As-made C-FDU-18 displays poor SAXS pattern (Figure 2A), which is probably caused by the low contrast between PEO-*b*-PS template and phenolic resin frameworks. After pyrolysis at 450 °C under N_2 atmosphere, the SAXS pattern becomes well-resolved. Four scattering peaks with q-values of 0.206, 0.398, 0.476, 0.710, 0.981, and 1.21 nm are clearly observed. These peaks can be exactly indexed to the 111, 311, 400, 440, 644 (or 820), and 862 reflections of highly ordered *fcc* mesostructure with the space group of $Fm\bar{3}m$. The cell parameter (a) is calculated to be 52.8 nm, indicating an ultralarge unit. After calcination at 800 °C, the well-resolved SAXS pattern is retained, suggesting that the highly ordered mesostructure is thermally stable. The cell parameter is as large as 46.4 nm, reflecting 12% shrinkage of the framework. Further increasing the heating temperature to 900 °C does not destroy the mesostructure. The ordered *fcc* mesostructure with a cell parameter of 45.0 nm can also be observed, and the framework shrinkage is minor (3.0%), suggesting a stable and rigid carbon framework.

TEM images and corresponding Fourier diffractograms (Figure 3) show that C-FDU-18 calcined at 800 °C under N_2 has a high degree of periodicity over large domains, viewed from the [100], [110], and [211] directions. It further confirms that the carbon mesostructure templated by diblock copolymer

(30) Broekhoff, J. C. P.; deBoer, J. H. *J. Catal.* **1967**, *9*, 8.

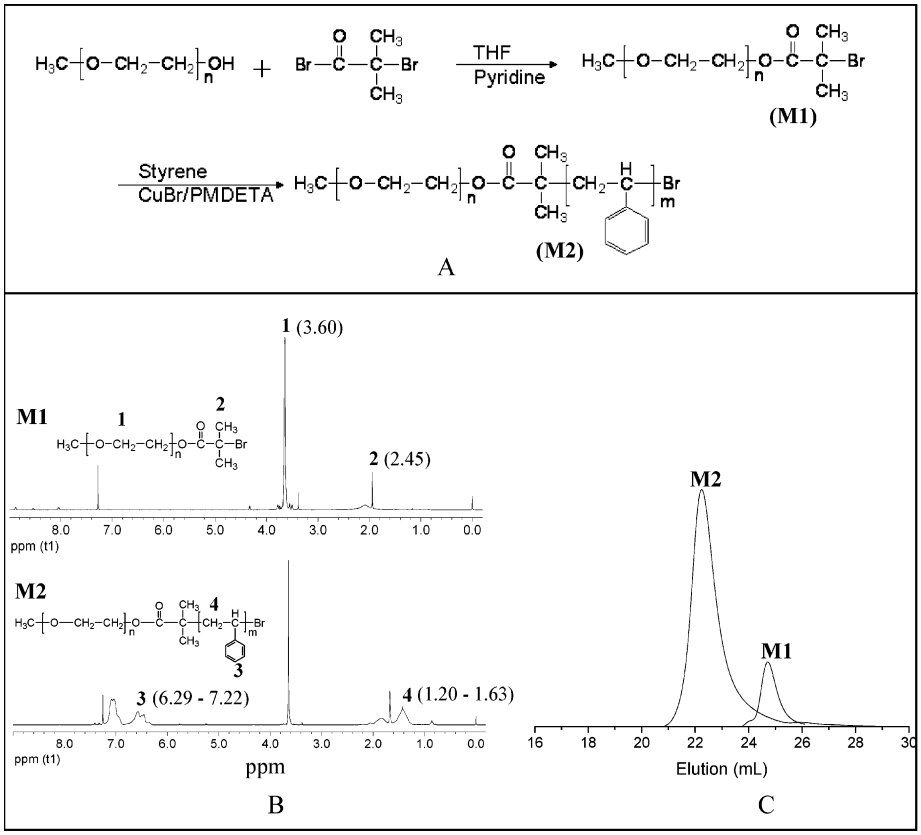

Figure 1. (A) Synthetic route for PEO-*b*-PS via ATRP, (B) ^{1}H NMR spectra, and (C) GPC traces of PEO-Br (**M1**) and diblock copolymer PEO-*b*-PS (**M2**).

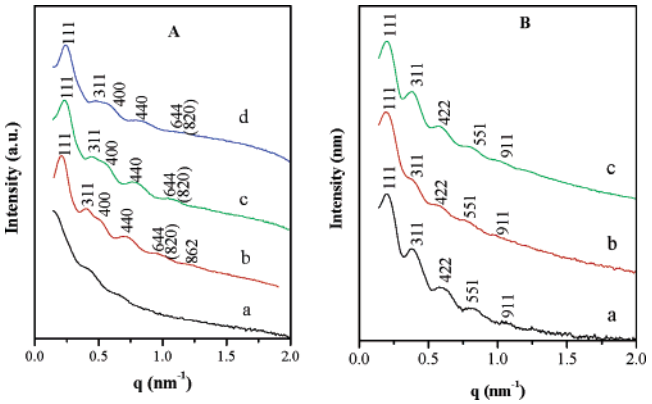

Figure 2. Panel A shows the SAXS patterns of as-made C-FDU-18 (a), C-FDU-18-450 pyrolyzed at 450 °C in N_2 (b), C-FDU-18-800 pyrolyzed at 800 °C in N_2 (c), and C-FDU-18-900 pyrolyzed at 900 °C in N_2 (d). Panel B shows the SAXS patterns of as-made Si-FUD-18 (a), Si-FDU-18-H obtained after the hydrothermal recrystallization of Si-FUD-18 at 100 °C for 3 days (b), and Si-FDU-18-HC obtained after further calcination of trace b at 600 °C for 6 h in air (c).

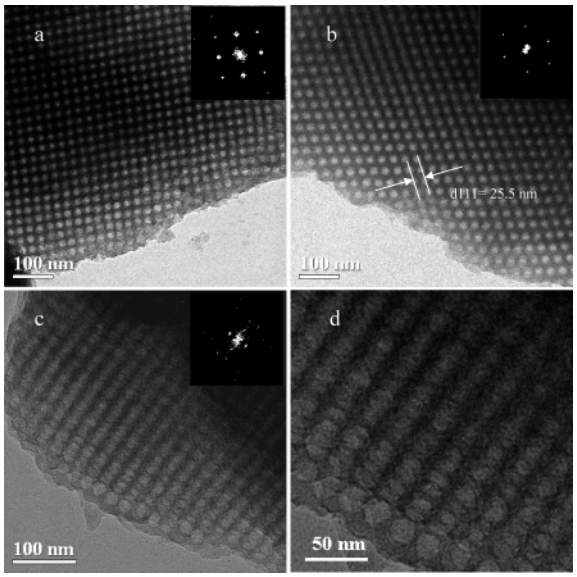

Figure 3. TEM images of mesoporous carbon C-FDU-18-800 pyrolyzed at 800 °C in N_2 viewed from the [100] (a), [110] (b), and [211] (c,d) directions. The image in panel d is the enlarged image of that in panel c. Insets are corresponding FFT diffractograms.

PEO_{125}-PS_{230} has a highly ordered cubic (*fcc*) symmetry. The uniform and spherical large mesopores are clearly visible in these images. This phenomenon implies the spherical packing from monodispersed PEO_{125}-PS_{230} globular micelles during the EISA process. The cell parameter of C-FDU-18-800 estimated from TEM images is about 45.6 nm, in good agreement with that from the SAXS pattern. TEM images also show that the wall thickness is rather thick, roughly measured to be about 9.0 nm.

N_2 sorption isotherms (Figure 4A) of mesoporous C-FDU-18-450 behave like representative type IV curves with a sharp capillary condensation step in the relative pressure range of 0.85−0.95. It indicates the generation of mesopores with an ultralarge uniform size. A very large H_2-type hysteresis loop with delayed capillary evaporation located at a relative pressure of about 0.5 is observed in the isotherms, implying caged mesopores with a window size smaller than 5.0 nm. It should be noted that the adsorption and desorption isotherms of FDU-18-450 are not close at low relative pressure, which may be related to the organic polymer materials.[31] On the basis of the

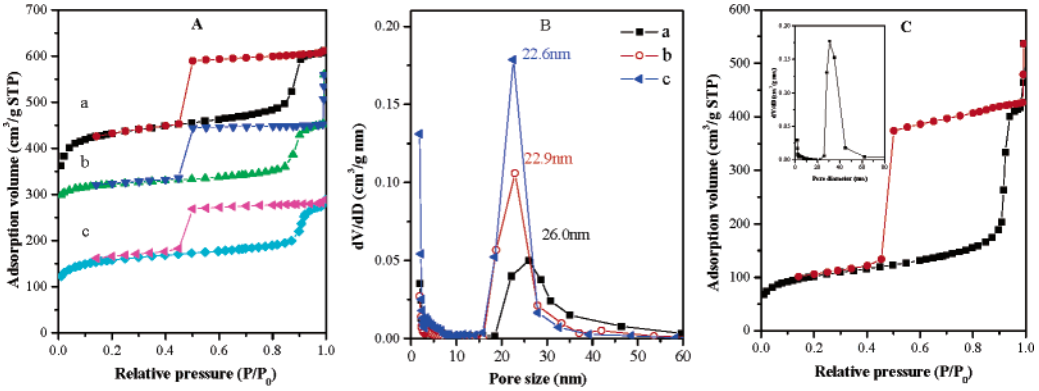

Figure 4. (A) N_2 adsorption−desorption isotherms and (B) pore size distribution curves of C-FDU-18-450 pyrolyzed at 450 °C in N_2 (a), C-FDU-18-800 pyrolyzed at 800 °C in N_2 (b), and C-FDU-18-900 pyrolyzed at 900 °C in N_2 (c). The N_2 adsorption−desorption isotherms of C-FDU-18-800 is vertically upset by 100 cm^3/g. (C) N_2 adsorption−desorption isotherms of mesoporous silica Si-FDU-18-HC prepared by using PEO_{125}-*b*-PS_{230} as a template via EISA followed by hydrothermal treatment at 100 °C for 3 d and calcination at 600 °C for 6 h in air. The inset is the pore distribution determined by the BdB sphere model.

Table 1. Textual Properties of the Mesoporous Carbon and Silica Products[a]

sample name	d_{111} (nm)	*a* (nm)	pore size (nm)	wall thickness (nm)	BET surface area (m^2/g)	micropore surface area (m^2/g)	pore volume (cm^3/g)	micropore volume (cm^3/g)
C-FDU-18-450	30.5	52.8	26.0	11.3	554	353	0.45	0.16
C-FDU-18-800	26.8	46.4	22.9	9.91	770	638	0.71	0.29
C-FDU-18-900	26.0	45.0	22.6	9.22	1510	1220	0.95	0.54
as-made Si-FDU-18	31.5	54.6						
Si-FDU-18-H	32.7	56.7						
Si-FDU-18-HC	31.4	54.4	30.8	7.66	362	140	0.66	0.06

[a] The *d*-spacing values were calculated by the formula $d = 2\pi/q$, and the unit cell parameters were calculated from the formula $a = d_{111}\sqrt{3}$. The wall thickness values were calculated from $W_T = \sqrt{2}a/2 - D$, where *a* represents the cell parameter and *D* is the pore diameter.

Broekoff-de Boer (BdB) sphere model, the mean pore size measured from the adsorption branch is as large as 26.0 nm (Figure 4B). The BET surface area and pore volume are 353 m^2/g and 0.45 cm^3/g, respectively (Table 1). Similar isotherms with very large H_2-type hysteresis loops can also be detected for C-FDU-18-800 and C-FDU-18-900 pyrolyzed at high-temperature (800 and 900 °C), suggesting that uniform, large, caged pores with a small opening are retained. The mean pore sizes (Figure 4B) of C-FDU-18-800 and C-FDU-18-900 calculated from the BdB sphere model are similar, which are 22.9 and 22.6 nm, respectively, and are slightly smaller than that of FDU-18-450. These results are in accordance with that from the SAXS pattern. The structural shrinkage is small when the heating temperature ranges from 800 to 900 °C. Notably, the BET surface area of C-FDU-18-900 is 1510 m^2/g, much larger than that of C-FDU-18-800. This may be caused by the continuous removal of carbon, hydrogen, and oxygen from the thick walls during pyrolysis. The *t*-plot calculation reveals that the micropore surface area of C-FDU-18-900 is 1220 m^2/g, almost twice as large than that of C-FDU-18-800. It suggests that this process mainly brings about micropores. In fact, micropores are generated at lower temperature evidenced by the difference in micropore surface areas between C-FDU-18-450 and C-FDU-18-800. These phenomena demonstrate that micropores are generated during the carbonization and become distinctly large at 900 °C. Based on the N_2 sorption and SAXS results, the wall thickness of mesoporous C-FDU-18 templated by PEO_{125}-PS_{230} is very thick, ranging from 9.2 to 11.3 nm and declines with the increase of pyrolysis temperature (Table 1). The values coincide with that from the TEM measurements. The thick walls and large pore dimensions for ordered mesoporous carbon are related with superlong polymer chains of templates, which was rarely reported before.

The TGA curve (Figure S3) of as-made C-FDU-18 shows several obvious weight-loss stages. The weight losses below 430 °C may be assigned to the desorption of solvents, the dehydration of numerous hydroxyl groups, and the decomposition of the PEO_{125}-PS_{230} template. The weight loss between 430 and 800 °C is about 40 wt %, which can be ascribed to the carbonization of frameworks. A minor weight loss (ca. 3 wt %) is observed between 800 and 900 °C, suggesting a continuous removal of carbon, hydrogen, and oxygen. The carbonization yield based on phenol resins is about 32 wt %. Elemental analysis of C-FDU-18-450 reveals that the framework is composed of C (76.8 wt %), H (4.5 wt %), and O (15.6 wt %) with a C/H/O molar ratio of 6.6:4.6:1, which is similar to the composition of phenolic resins. C-FDU-18-800 possesses a molar ratio for C/H/O of 16.2:3.6:1, indicating that the carbon frameworks are produced. Raman spectra (Figure S4) of C-FDU-18-800 and C-FDU-18-900 show a G band at 1591 cm^{-1} and a D band at 1313 cm^{-1} with comparable intensities. Because the G band is related with graphitic sp^2 carbon structures and the D band is associated with defective sp^2 carbon structures, we can conclude that the obtained carbon materials have a low degree of graphitization. FTIR spectra (Figure S5) further identify the polymer feature framework of C-FDU-18-450 and carbon framework of C-FDU-18-800.

3.3. Large-Pore Ordered Mesoporous Silicas (Si-FDU-18). The laboratory-made diblock copolymer PEO_{125}-PS_{230} is thereafter used as the template to synthesize highly ordered meso-

(31) McKeown, N. B.; Budd, P. M.; Msayib, K. J.; Ghanem, B. S.; Kingston, H. J.; Tattershall, C. E.; Makhseed, S.; Reynolds, K. J.; Fritsch, D. *Chem.—Eur. J.* **2005**, *11*, 2610.

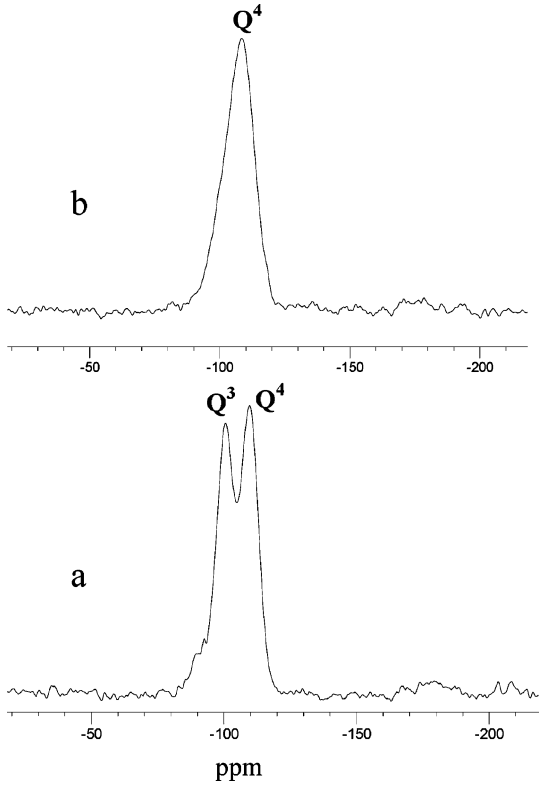

Figure 5. ^{29}Si solid-state NMR spectra of as-made mesoporous silica Si-FDU-18 before (a) and after (b) the hydrothermal treatment.

porous silica via the EISA strategy. Unfortunately, the products directly calcined at 600 °C in air show BET surface area near to zero. To solve the problem, an efficient hydrothermal recrystallization treatment at 100 °C for 3 days was adopted.

The SAXS pattern (Figure 2B) for as-made mesoporous silica Si-FDU-18 prepared by using diblock copolymer PEO_{125}-PS_{230} as a template via the EISA approach under an acidic condition shows five resolved diffraction peaks. It is similar to that of C-FDU-18-800, suggesting that mesoporous silica possesses the same mesostructure as C-FDU-18. These five peaks can be indexed to 111, 311, 422, 551, and 911 reflections associated with the *fcc* mesostructrure ($Fm\bar{3}m$). The calculated cell parameter is 54.6 nm, even larger than that of as-made C-FDU-18. After the hydrothermal recrystallization at 100 °C for 3 days, the four well-resolved scattering peaks can also be detected for the resultant Si-FDU-18-H with a slight shift to low q values. It manifests the maintenance of a highly ordered mesostructure accompanied by the enlargement of the unit cell possibly caused by the expansion of PEO-*b*-PS upon the hydrothermal treatment. After calcination at 600 °C in air, the well-resolved SAXS pattern is retained, indicating that the highly ordered *fcc* Si-FDU-18-HC mesostructure is thermally stable. The cell parameter is 54.4 nm, which is much larger than that of C-FDU-18-800 and represents a minor framework shrinkage of 4%. It is related to the nature of frameworks. ^{29}Si solid-state NMR spectrum (Figure 5a) of as-made Si-FDU-18 shows two bands associated with Q^3 and Q^4 silicate species, suggesting a large number of silanol groups. After the hydrothermal treatment, the obtained Si-FDU-18-H displays only one broad Q^4 band at 110 ppm (Figure 5b). It clearly indicates that further cross-linkage and condensation of the silicate frameworks occur. These phenomena demonstrate that the rigid and fully cross-linked

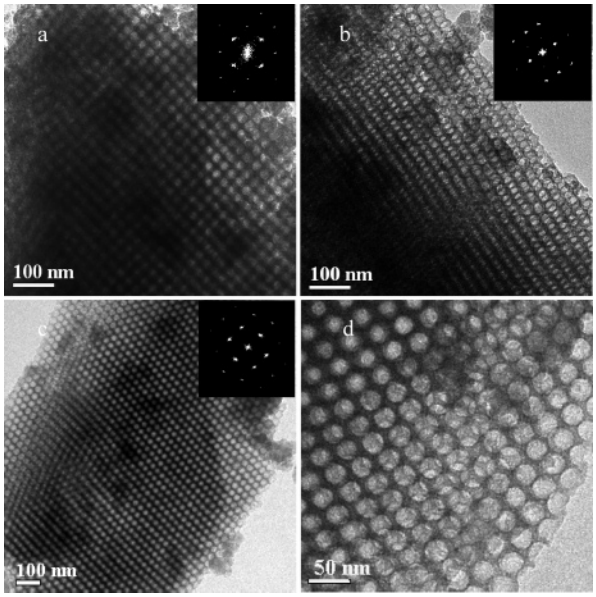

Figure 6. TEM images of calcined mesoporous silica Si−FDU-18-HC after hydrothermal treatment at 100 °C for 3 days and calcination at 600 °C for 6 h in air viewed from the [100] (a), [211] (b), and [411] (c,d) directions, respectively. The image in panel d is the enlarged image of that in panel c. Insets are corresponding FFT diffractograms.

silica frameworks have been formed during the hydrothermal recrystallization and hence can resist the shrinkage upon calcination.

TEM images (Figure 6) of Si-FDU-18-HC show large-domain regularity, indicating a highly ordered mesostructure. The images taken from the [100], [211], and [411] directions with corresponding FFT diffractograms further confirm a 3-D cubic ($Fm\bar{3}m$) symmetry. The cell parameter estimated from TEM images is about 51.2 nm, consistent with the value from the SAXS data. Similar to that for C-FDU-18-800, the spherical closed packing morphology can be clearly observed from the images (Figure 6b,d). The dissimilarity between these two materials is structural defects which can be observed in some small domains for Si-FDU-18-HC (Figure S6). This phenomenon can be explained by the interference of ethanol with the silica-copolymer assembly. Ethanol is released by the hydrolysis of TEOS which is a precipitator for PEO-*b*-PS diblock copolymers.

Si-FDU-18-HC exhibits similar N_2 sorption isotherms (Figure 4C) to C-FDU-18-800. The type IV curves with a capillary condensation step at very high relative pressure ($P/P_0 = 0.87-0.95$) and a very large H_2-type hysteresis loop suggest ultralarge uniform mesopores with a small opening window. A narrow pore size distribution centered at 30.8 nm can be obtained from the adsorption branch by the BdB model (inset of Figure 4C). To the best of our knowledge, it is so far the largest pore size for highly ordered mesoporous silicates. Mesoporous silica Si-FDU-18-HC possesses a BET surface area of 362 m^2/g. The *t*-plot analysis shows the micropore surface area of 140 m^2/g, much smaller than those in calcinated C-FDU-18. These results demonstrate that mesoporous silica has less microporosity. The silica pore wall thickness calculated from the N_2 sorption and SAXS data is very thick ($\sim$ 7.7 nm) which may be due to the long EO chain of the template.

The sample (donated as Si-FDU-18-C) prepared from direct calcinations of as-made Si-FDU-18 without prior hydrothermal

Scheme 1. Schematic Illustration for the Formation Processes of Highly Ordered Mesoporous Carbon (C-FDU-18) and Silica (Si-FDU-18) with Large Accessible Pores.

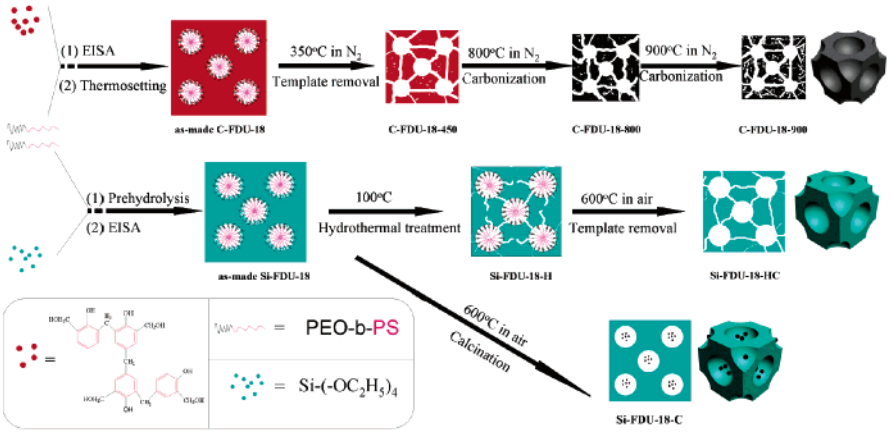

treatment is gray and black, which is much different from the white color for Si-FDU-18-HC (Figure 7). These phenomena can be attributed to the incomplete decomposition of PEO-*b*-PS template in the former, and carbon deposition occurs. Si-FDU-18-C shows almost no N_2 adsorption at relative pressure of 0−1 and exhibits a BET surface area near zero, indicating that the pores are not opened. To understand the pore structure, the as-made Si-FDU-18 was heated to above 400 °C in air, followed by a dissolving of the silica frameworks with HF. Instead of the clear solution, black suspensions were produced. TEM measurements show that the suspensions comprise a large number of carbon nanoparticles (Figure S7), which confirms that the PEO-*b*-PS templates were carbonized in pores rather than eliminated. Similar results have been previously reported by Yu et al.[16] They tried to prepare cubic mesoporous silica by using diblock copolymer PS-*b*-PEO as a template which was derived from sequential anionic polymerization of styrene and ethylene oxide. N_2 sorption measurements performed on a surface acoustic wave (SAW) device also showed no nitrogen adsorption at relative pressures lower than 0.8. It implies closed pores in mesoporous silicas. A model can be established as the mesopores are isolated with each other and separated by the thick and condensed silica walls. The pore wall thickness may be close to the value in Si-FDU-18-HC (~7.7 nm) with a little fluctuation on the consideration of condensation of silanol groups. The gas molecules are not allowed to go through (in or out) the thick walls. Consequently, organic template molecules undergo carbonization in the pores and N_2 molecules cannot penetrate through the walls into the cages. It brings about a zero BET surface area.

Elemental analysis exhibits that as-made Si-FDU-18 contains C and H with the content of 20.4 and 3.8 wt %, respectively,

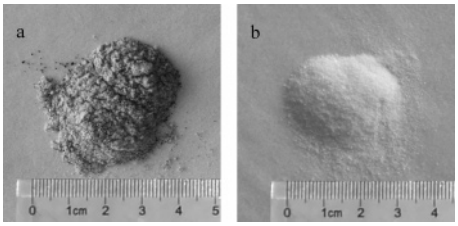

Figure 7. Photograph images of Si-FDU-18-C (a) obtained by direct calcination of the as-made FDU-18 in air, and Si−FDU-18-HC (b) obtained after hydrothermal treatment and further calcination at 600 °C in air for 6 h.

while as-made Si-FDU-18-H from the hydrothermal treatment is composed of C (13.5 wt %) and H (2.8 wt %). These results suggest a considerable loss of organic species from the pore cages during the process of hydrothermal recrystallization. As-made Si-FDU-18 exhibits three weight-loss stages (Figure S8a). The first minor one of 8 wt % occurs between 25 and 200 °C, which can be assigned to the loss of physically absorbed water and solvents. In the temperature ranges from 200 to 450 °C and from 450 to 900 °C, 12 and 16 wt % weight losses are detected, respectively. They can be related to the decomposition and carbonization of PEO-*b*-PS template and the dehydration of silanol groups.[32] The weight-loss stages for Si-FDU-18-H occur in the similar temperature ranges but with different amounts (Figure S8b). The first and the third ones are minor, that is, 5 and 8 wt %, respectively. While the large weight loss (27 wt %) is observed between 200 and 450 °C, mainly caused by the decomposition of PEO-*b*-PS template. Considering the loss of organic template species and condensation of silanol groups during the hydrothermal treatment, the total weight loss of Si-FDU-18-H is much higher than that for Si-FDU-18 without the hydrothermal treatment. It may be the secondary evidence that the templates in mesoporous silica can be released by calcination after the hydrothermal treatment.

The successful synthesis of ultralarge pore mesoporous carbons and silicas with highly ordered *fcc* structure is primarily attributed to the PEO-*b*-PS template with high molecular weight, in particular, to the long hydrophobic PS segment. A schematic illustration for the synthesis is presented in Scheme 1. For the preparation of mesoporous carbon, the resol precursors can interact with the PEO segment of the diblock copolymer by hydrogen bonding. The PEO-*b*-PS/resols mesostructure is formed by organic−organic self-assembly during the solvent evaporation. Upon thermosetting at 100 °C, the framework polymerizes, casting the mesostructure of PEO-*b*-PS micelles. It should be noted that the polymerizing processes of the phenolic resin frameworks separate from the assembly process of PEO-*b*-PS and resols. The polymer frameworks further cross-link and dehydrogenate during the subsequent pyrolysis with the maintenance of the highly ordered mesostructure. A great amount of carbon, hydrogen, and oxygen is decomposed and

(32) Huo, Q.; Margolese, D. I.; Ciesla, U.; Demuth, D. G.; Feng, P.; Gier, T. E.; Sieger, P.; Firouzi, A.; Chmelka, B. F.; Schuth, F.; Stucky, G. D. *Chem. Mater.* **1994**, *6*, 1176.

escapes from the frameworks. It results in a large structural shrinkage and leaves many voids. Micropores are generated to connect the primary mesopores. The PEO-*b*-PS copolymer template can be decomposed and removed from these pores, and nitrogen molecules can adsorb inside the pores. Therefore, highly ordered mesoporous carbon frameworks with large accessible pores and high surface areas can be easily fabricated.

Different with mesoporous carbons, the silica mesostructure is formed by a cooperative organic-inorganic assembly of the diblock copolymer PEO-*b*-PS and silicate species. During the mesostructure formation, the cross-linking and condensation of silicate species simultaneously occur. The PEO-*b*-PS copolymer gets a compact packing of globular micellar aggregate surrounded by thick silicates owing to extreme hydrophobicity and strong aggregation of the long PS chain. As a result, the PEO segment covalently linked with PS chain gradually retracts from silica walls.[16] Further cross-linkage yields condensed silica walls upon calcination. PEO-*b*-PS templates can be partially decomposed and carbonized inside the isolated pore cages. The silica products have thick pore walls without voids, as well as large closed mesopore cages inaccessible with N_2 gas.

In contrast, the PEO-*b*-PS templates vigorously swell caused by the withdrawal of the PEO segment and thermal movements of both segments during the high-temperature (100 °C) hydrothermal treatment. Simultaneously, silica frameworks undergo reorganization and recrystallization via further cross-linkage and condensation, which would result in a large structural shrinkage. The intense confliction may eventually lead to cracking of the silica walls and micropores that link the large caged mesopores. The mesopore cages are therefore accessible with gas molecules.

In conclusion, we demonstrate a successful synthesis of highly ordered mesoporous carbons and silicas both with ultralarge accessible pores by using high molecular weight PEO-*b*-PS copolymer as a template via the EISA strategy. Mesoporous carbon and silica products (FDU-18) have large-domain ordered *fcc* closed-packing ($Fm\bar{3}m$) mesostructure with a superlarge lattice of up to 46.4 and 54.4 nm, respectively. N_2 sorption isotherms show that mesoporous carbon has a uniform large pore size of ∼23 nm, high BET surface area of ∼1510 m^2/g, and pore volume of 0.95 cm^3/g which mainly contributes from micropores. The spherical pore cages of Si-FDU-18 are isolated by very thick walls, resulting in inaccessible pores by small gas molecules as reported previously. An efficient hydrothermal recrystallization is adopted for the first time to make the ultralarge pores (30.8 nm) open and accessible by producing microporosity on the thick silica walls (∼7.7 nm). The ultralarge pores with different components in walls, such as polymer, carbon, and silica are appealing in various applications including electrode materials, adsorption, catalysis, and photonic waveguide, etc. In addition, the laboratory-made block copolymer PEO-*b*-PS is easily available because of the simplicity of the ATRP method. It is feasible in the templating synthesis of large-pore mesoporous materials with abundant compositions such as metal oxides.

Acknowledgment. This work was by NSF of China (Grant Nos. 20233030, 20421303, 20407014, 20373013, 20641001 and 20521140450), Shanghai Sci. & Tech. Committee (Grant Nos. 06DJ14006, 055207078, 05DZ22313, 04JC14087), State Key Basic Research Program of PRC (Grant No. 2006CB202502), Shanghai Nanotech Promotion Center (Grant No. 0652nm024) and Shanghai HuaYi Chemical Group. Y.H.D. thanks China Postdoctoral Scientific Fund and Shanghai Postdoctoral Scientific Program.

Supporting Information Available: FTIR spectra of PEO5000, PEO-Br, and PEO-*b*-PS diblock polymer, TGA of PEO-*b*-PS and PEO-*b*-PS/resols composites (as-made C-FDU-18), Raman spectra of C-FDU-18-800 and C-FDU-18-900, FTIR spectra of as-made C-FDU-18, C-FDU-18-450 and C-FDU-18-800, and TEM image of Si-FDU-18-HC obtained with hydrothermal treatment after calcination in air at 600 °C. This material is available free of charge via the Internet at http://pubs.acs.org.

JA067379V